Influence of non-stoichiometry on the magnetic properties of magnetite nanoparticles

2008 J. Phys.: Condens. Matter 20 195213

(http://iopscience.iop.org/0953-8984/20/19/195213)

IOP Publishing Journal of Physics: Condensed Matter

J. Phys.: Condens. Matter **20** (2008) 195213 (6pp) doi:10.1088/0953-8984/20/19/195213

Influence of non-stoichiometry on the magnetic properties of magnetite nanoparticles

J Mazo-Zuluaga[1], J Restrepo[1] and J Mejía-López[2]

[1] Grupo de Estado Sólido, Grupo de Instrumentación Científica y Microelectrónica, Instituto de Física, Universidad de Antioquia, A A 1226 Medellín, Colombia
[2] Facultad de Física, Pontificia Universidad Católica, Avenida Vicuña Mackenna 4860, Santiago, Chile

E-mail: jomazo@fisica.udea.edu.co, jrestre@fisica.udea.edu.co and jmejia@puc.cl

Received 15 February 2008, in final form 14 March 2008
Published 11 April 2008
Online at stacks.iop.org/JPhysCM/20/195213

Abstract

In this study we investigate the magnetic properties of magnetite fine particles using Monte Carlo simulation in the framework of a core–shell model. A single-spin movement Metropolis dynamics was implemented to compute equilibrium averages. Calculations were performed on the basis of a three-dimensional classical Heisenberg Hamiltonian, with nearest magnetic neighbour interactions, and taking into account three different superexchange integrals associated to iron cations of tetrahedral and octahedral sites. The Hamiltonian includes a surface anisotropy term applied to surface ions, and cubic anisotropy for ions belonging to the core. Different diameters were considered in order to figure out different off-stoichiometric scenarios and the influence on the magnetic properties. Results reveal a well-defined power law particle size dependence of the Curie temperature, characterized by an exponent $\nu = 0.82(5)$. No evidence for surface spin disorder was detected. Finally, susceptibility data reveal that the ferrimagnetic-to-paramagnetic transition occurs in a gradual fashion ascribed to a differentiated behaviour between the core and surface.

(Some figures in this article are in colour only in the electronic version)

1. Introduction

The surface of magnetite has been studied intensively over the past decade and much of the work has been focused on the potential use of magnetite for spintronics applications [1]. It is one of the few materials with a very high degree of spin polarization at the Fermi level that possesses a high Curie temperature (∼859 K) and exhibits a metal-to-insulator transition better known as the Verwey transition [2]. Since spintronics involves electron transport across or along a material interface, an understanding of the structure, electronic, and magnetic properties of the surface is a key issue for making progress in this area and in those where surface effects play an important role. Such effects involve changes in the coordination number, presence of uncompensated spins due to the breaking of symmetry at the surface, deviations from ideal stoichiometry, etc. In the case of nanoparticles, surface effects are more pronounced as the particle size diminishes and other aspects like the magnetization and the density of states are strongly dependent on the specific way in which the surface ends. In particular, five different terminations of the $Fe_3O_4(111)$ surface were studied in the framework of density functional theory with the generalized gradient and local density approximation $+U$ approaches, where magnetization was significantly affected by the type of termination [3]. Such terminations are characterized by under-coordination and missing bonds, which induce stoichiometry inhomogeneities. On the other hand, the Verwey transition in stoichiometric magnetite has been shown to change its discontinuous character to a continuous one while changing the non-stoichiometric parameter δ in $Fe_{3-\delta}O_4$ [4]. More specifically, the transition temperature decreases with increasing deviations from ideal Fe:O stoichiometry of less than 0.3%. With larger deviations, the transition changes to second order and finally it disappears at about 1% deviation [4]. Moreover, the limit for passing from a first-order phase

transition to a higher-order transition has been set to $\delta = 0.0039$ [5]. This may be the reason for the shift of T_V observed in some magnetite nanoparticles (96 K), which is lower than that of bulk magnetite (∼120 K) [6]. Non-stoichiometry could also be the reason why the Verwey transition has not been observed in other magnetite nanoparticle systems [7, 8]. Hence, the question as to whether there is or is not a Verwey transition in nanosized magnetite seems to be still open. More recently, experimental evidence using conversion electron Mössbauer spectroscopy and x-ray magnetic circular dichroism on ultrathin $Fe_{3-\delta}O_4$ (111) films grown epitaxially on Pt(111) has demonstrated the paramount importance of non-stoichiometry as a driving force of the magnetic and electric properties of magnetite at nanometric scales [9]. Experimental evidence has also endorsed both the occurrence of surface spin disorder, as well as the idea of a core–shell model as the mechanism responsible for magnetization reduction [10]. Hence, the scenario of a state where surface spins become canted and oriented along directions different from those ruled out by internal magnetocrystalline anisotropy has been postulated [8].

In this paper, we address the magnetic properties of $Fe_{3-\delta}O_4$ magnetite nanoparticles by using Monte Carlo simulation in the framework of a classical Heisenberg spin model. Different nanoparticle sizes have been simulated in order to reproduce different stoichiometric scenarios with large surface-to-volume ratios.

2. Model and simulation details

Magnetite is a ferrimagnetic compound with inverse spinel structure having Fe^{3+} and Fe^{2+} ions distributed in two sublattices with different O^{2-} coordination [11]. Its structure (space group *Fd3m* with 32 oxygen and 24 iron ions per unit cell) consists of eight tetrahedral positions (A sublattice) occupied by Fe^{3+} ions and 16 octahedral sites (B sublattice) having 8 Fe^{2+} and 8 Fe^{3+} ions randomly distributed. On this structural basis, magnetite nanoparticles, with a closely spherical shape, were simulated by implementing free boundary conditions, and diameters were considered up to 10.0 nm. It must be stressed that the way the nanoparticle has been cut out from a cube might give rise to a surface structure that is slightly rough. Experimental evidence has demonstrated the occurrence of both well-defined faces in magnetite nanocrystals [12] as well as magnetite nanoparticles having a spherical shape in the size range considered in our study [13–22]. Relaxation effects and surface reconstruction were not taken into account and they are currently under investigation. The Heisenberg Hamiltonian describing the interactions in the system can be written as:

$$H = -2\sum_{\langle i,j\rangle} J_{ij}\vec{S}_i\cdot\vec{S}_j - K_S\sum_k(\vec{S}_k\cdot\hat{n}_k)^2 - K_V\sum_i(S_{x,i}^2S_{y,i}^2 + S_{y,i}^2S_{z,i}^2 + S_{x,i}^2S_{z,i}^2). \quad (1)$$

The first sum runs over nearest magnetic neighbours involving different coordination numbers, depending on the crystallographic site, which under bulk conditions are: $z_{AA} = 4$, $z_{BB} = 6$, $z_{AB} = 12$, and $z_{BA} = 6$. A surface was defined as being formed by those ions having coordination numbers smaller than those for the bulk system. Magnetic ions Fe_A^{3+}, Fe_B^{3+}, and Fe_B^{2+} were represented by classical Heisenberg spins ($S = 5/2$ for Fe^{3+} and $S = 2$ for Fe^{2+}), whereas oxygen ions were considered as non-magnetic. The second term accounts for the single-ion site surface anisotropy and the unit vector on the surface at each $\vec{P}_i$ position is computed using the following expression [10]:

$$\hat{n}_i = \sum_j\left(\vec{P}_i - \vec{P}_j\right)\Big/\left|\sum_j\left(\vec{P}_i - \vec{P}_j\right)\right|, \quad (2)$$

where the sum runs over nearest magnetic neighbours surrounding the ith ion. The third term in (1) gives the core cubic magnetocrystalline anisotropy, with constant $K_V = 0.002$ meV/spin [8]. Numerical values of the integrals employed were $J_{AA} = -0.11$ meV, $J_{AB} = J_{BA} = -2.92$ meV, and $J_{BB} = +0.63$ meV [23], whereas a value of $K_S/K_V = 10$ was assigned to the anisotropy constant ratio [24]. A single-spin movement Metropolis Monte Carlo algorithm for computing equilibrium thermodynamic properties was employed. The bulk system was also simulated using periodic boundary conditions and a linear system size $L = 10$, with a total number of magnetic ions $N = 24 \times L^3$.

Up to five different realizations of Fe^{3+} and Fe^{2+} at octahedral sites, and around 7×10^5 Monte Carlo steps per spin (mcs), were considered for computing equilibrium averages. The first 4×10^5 configurations were discarded for equilibration. The equilibrium thermodynamic quantities computed were total energy, magnetization per spin, magnetic susceptibility, and heat capacity. Magnetization was computed according to the following relationship:

$$\langle|m|\rangle = \frac{1}{N(\mathrm{MCS}_{\max} - n_O)}\sum_{i=n_O+1}^{\mathrm{MCS}_{\max}}\left(\vec{M}_i\cdot\vec{M}_i\right)^{1/2}, \quad (3)$$

where:

$$\vec{M}_i\cdot\vec{M}_i = M_i^2 = \left[\left(\sum_{j=1}^{N}S_{jx}\right)^2 + \left(\sum_{j=1}^{N}S_{jy}\right)^2 + \left(\sum_{j=1}^{N}S_{jz}\right)^2\right]_i. \quad (4)$$

Here, N is the total number of Fe cations, n_O is the number of configurations discarded for equilibration, and $\mathrm{MCS}_{\max}$ is the total number of Monte Carlo steps. Magnetic contributions to the total magnetization per magnetic site from surface, core, A, and B sites, were also explicitly computed. Analogously, the same contributions to the magnetic susceptibility were also obtained.

3. Results and discussion

In order to quantify the degree of stoichiometry in $Fe_{3-\delta}O_4$ nanoparticles, for every system size, the oxidation parameter (δ) was computed according to:

$$\delta = 3 - \frac{4N_T(\mathrm{Fe})}{N_T(O^{2-})}, \quad (5)$$

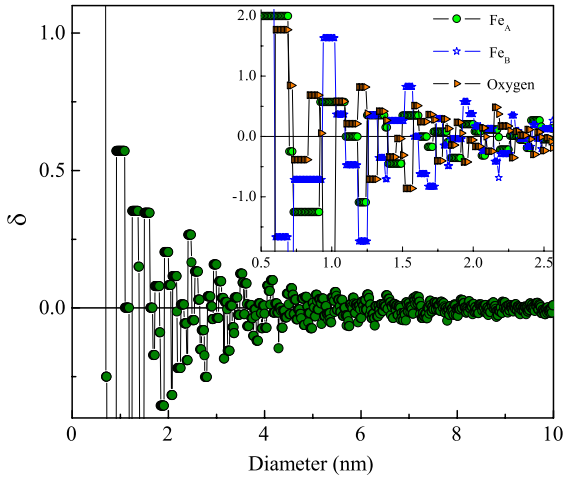

Figure 1. Diameter dependence of the oxidation parameter (δ). Inset shows the behaviour for very fine nanoparticles, when considering different locations of the centre (Fe_A, Fe_B and O^{2-}).

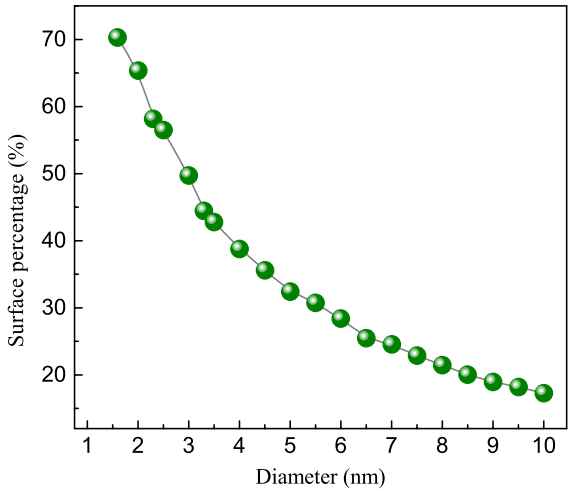

Figure 2. Percentage of surface Fe cations as a function of the nanoparticle diameter.

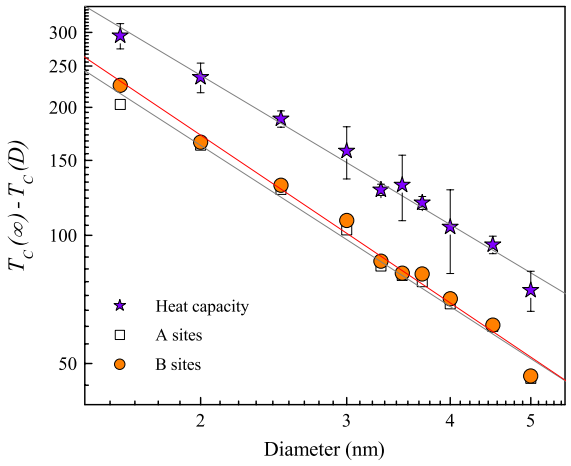

Figure 3. Diameter dependence of the difference between T_C for the nanoparticle and the bulk Curie temperature.

where $N_T(x)$ represents the total number of x-type ions. This expression gives the relative amounts of iron and oxygen ions in the system, and is independent of the way in which the Fe_B^{2+} and the Fe_B^{3+} are distributed on the octahedral sites. For stoichiometric bulk magnetite $\delta = 0$. Figure 1 shows the system size dependence of δ when considering the nanoparticle centred at a Fe_A^{3+} ion, whereas the inset shows an enlargement of such dependence when considering other centres. Depending on the choice of centre, nanoparticles with $\delta \approx 0$, as small as 1 nm, are observed.

On the other hand, independently of where the centre is, the δ parameter tends to zero as the nanoparticle size increases. Moreover, for diameters above 5 nm, nanoparticles exhibit a stoichiometry with $|\delta| \leqslant 0.1$ close to that of an ideal magnetite, which corresponds, in the upper limit, to a magnetite of the form $Fe_{2.9}O_4$. This fact agrees with a recent work where highly stoichiometric magnetite nanocrystals of 5.5 ± 1.4 nm were synthesized [6]. Below 5 nm, large deviations of the oxidation parameter are observed for smaller nanoparticles. Such deviations appear progressively larger as the nanoparticle size decreases. Here, since the Fe:O proportion in the core is the same as that of a bulk magnetite, such deviations are exclusively due to the under-coordination on the surface. Figure 2 shows the diameter dependence of the percentage of Fe cations on the surface, relative to the total number of Fe cations. For magnetite nanoparticles having a diameter lower than 3.0 nm, more than 50% of Fe cations belong to the surface and, hence, the magnetic properties should, in principle, be dominated by the surface.

As regards the magnetic properties and critical behaviour, the dependence of the Curie temperature (T_C) as a function of the diameter is shown in figure 3. Critical temperatures $T_C(D)$, for the different system sizes, were obtained by considering the maxima for both the heat capacity and the A and B contributions to the total magnetic susceptibility. Such a size dependence of T_C was fitted according to finite size scaling theory through the following relationship [25, 26]:

$$T_C(\infty) - T_C(D) = bD^{-1/\nu}, \qquad (6)$$

where $T_C(\infty) = 859(4)$ K has been found in our simulation for the bulk system under periodic boundary conditions. The best estimate of the ν exponent was $\nu = 0.82 \pm 0.05$. This mean value, greater than $\nu = 0.7048(30)$ for a pure three-dimensional (3D) Heisenberg magnet [26], can be ascribed to several reasons involving: (i) crossover of dimensionality from 3D towards a 2D-like system, and (ii) features affecting the universality class such as competitive interactions, symmetry breaking at the surface, random distribution of exchange integrals, etc [25]. As is clear, T_C is shifted to lower values as the nanoparticle size decreases. This finite size effect is attributed to the under-coordination of the cations on the surface and consequently to the smaller density of magnetic bonds.

In order to elucidate the influence of the non-stoichiometry on the magnetic properties, figure 4 shows the temperature dependence of the total magnetization and the respective core and surface contributions for some selected diameters. At low temperatures, the core contribution to the magnetization decreases when the nanoparticle diameter diminishes, whereas the surface contribution becomes dominant.

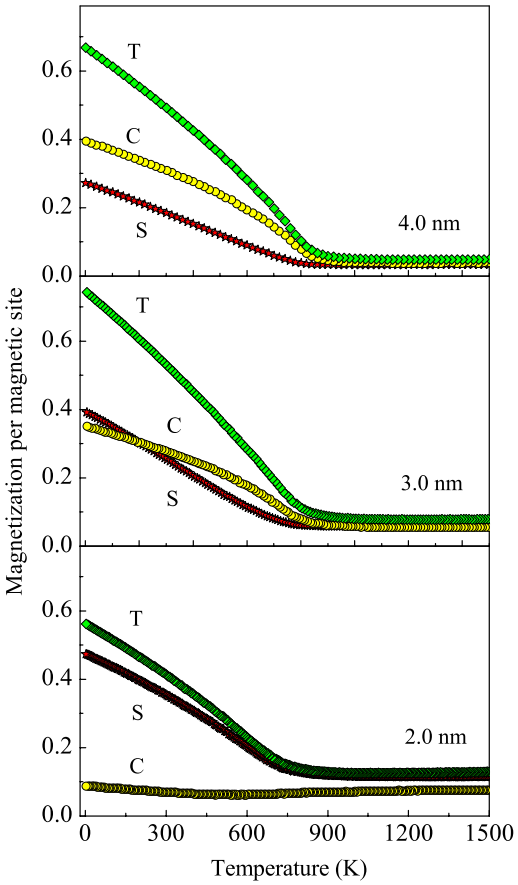

Figure 4. Temperature dependence of the total magnetization per magnetic site (T) for nanoparticles of 2.0, 3.0, and 4.0 nm in diameter. Contributions from core (C) and surface (S) are also included.

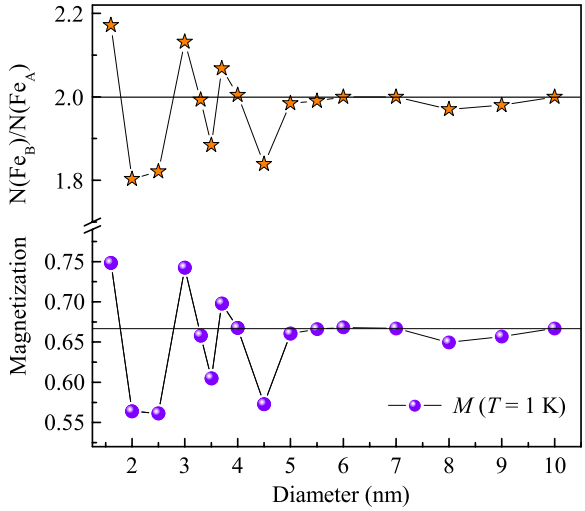

Figure 5. Bottom panel: magnetization per magnetic site evaluated at 1 K as a function of the system size. Top panel: system size dependence of the relative occupancy B:A.

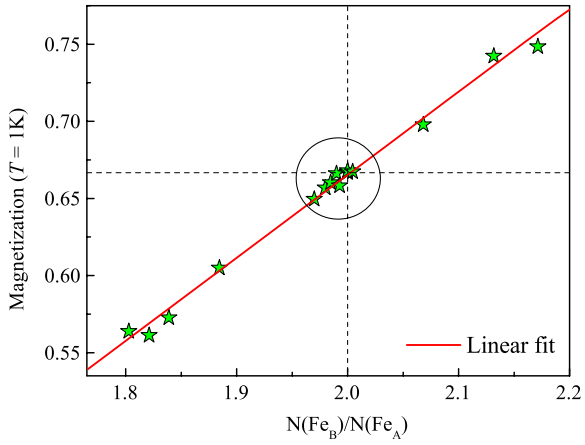

Figure 6. Linear dependence between the low-temperature magnetization and the relative B:A ratio. Dots within the circle correspond to those nanoparticles having stoichiometry closer to that of an ideal magnetite.

Our data reveal also a crossover between the core and surface contributions to the total magnetization at 3.0 nm, for which the percentages of atoms at the surface and the core are practically the same. At high temperatures above T_C, the tail observed in the magnetization, yields non-vanishing values, which are more noticeable for smaller nanoparticles. Hence, magnetizations per magnetic site both at the lowest temperature (1 K) and the highest one (1500 K) were evaluated. Figure 5 displays the magnetization evaluated at 1 K, in conjunction with the $[N(\mathrm{Fe}_B^{3+}) + N(\mathrm{Fe}_B^{2+})]/N(\mathrm{Fe}_A^{3+})$ ratio. As can be observed, both quantities follow the same oscillatory behaviour and hence a linear relationship is inferred (see figure 6). The straight line, resulting from a linear fit, passes through the point (2, 2/3) corresponding to the coordinates of a stoichiometric bulk magnetite. This simple fact implies the absence of surface spin disorder or any kind of spin canting. In consequence, a full antiparallel alignment between iron moments of A and B sublattices is concluded, at least for the values of anisotropy employed.

Figure 7 shows a snapshot of the spin surface configuration for the nanoparticle of 3.0 nm which is qualitatively the same in all cases. If any anomaly on the surface had taken place, involving canting or surface spin disorder, the resulting data were expected to lie below the straight line shown in figure 6, passing by a point different to (2, 2/3). It must be stressed that this scenario has been obtained with a relatively low K_S/K_V value, and the possibility of surface spin disorder for greater surface anisotropy values cannot be ignored.

Results shown in figure 5 reveal also the occurrence of a threshold diameter around 5.0 nm, below which off-stoichiometry is increasingly more noticeable. This fact is consistent with the values obtained for the oxidation parameter. Above this threshold, nanoparticles can be considered highly stoichiometric, and the magnetization per magnetic site at 1 K is very close to 2/3, corresponding to stoichiometric bulk magnetite.

Regarding the high-temperature behaviour, figure 8 shows the size dependence of the magnetization evaluated at 1500 K, well above the critical temperature. An interesting feature is the tendency of the magnetization to increase as the particle

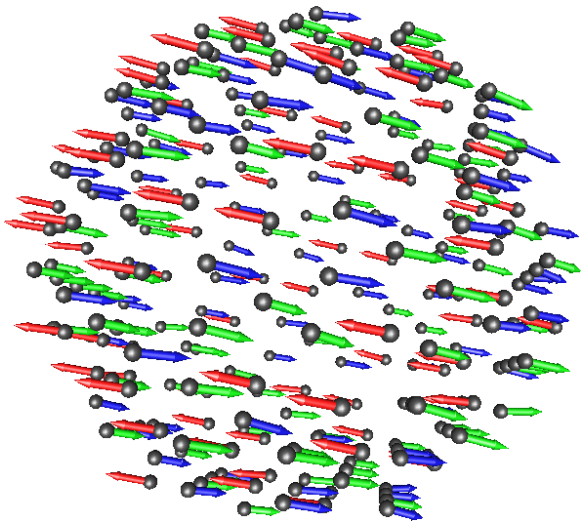

Figure 7. Surface spin configuration at 1 K for a 3.0 nm diameter nanoparticle. Arrows represent Fe spins: gray colour for Fe_A sites (pointing to the left), dark gray for Fe_B^{3+} ions and light gray for Fe_B^{2+} (both of them pointing to the right). Online version: red colour for Fe_A sites, blue colour for Fe_B^{3+} ions and green colour for Fe_B^{2+}.

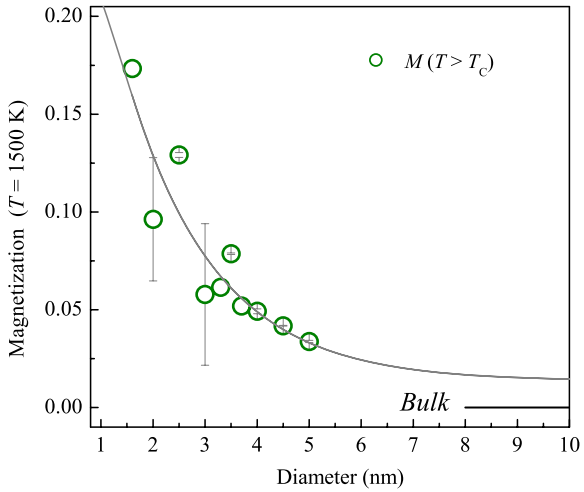

Figure 8. Total magnetization per magnetic site evaluated at 1500 K as a function of the particle size. A first-order exponential decay (grey line) has been carried out.

size decreases. Such behaviour indicates the occurrence of an uncompensated spin scenario and reveals clearly the interplay between off-stoichiometry and particle size. It must also be taken into account in this regard that the total magnetization per magnetic site is computed by considering the magnitudes of the magnetization vector at every Monte Carlo step (see (3)). As the particle size increases, the stoichiometry improves, spins become compensated, and the magnetization tends to zero.

Finally, in order to gain a deeper insight in the way the nanoparticles undergo the magnetic phase transition from the paramagnetic to the ferrimagnetic state, figure 9 shows the temperature dependence of the magnetic susceptibility, computed from the fluctuations in the magnetization, as well as the core and surface contributions. Data are displayed

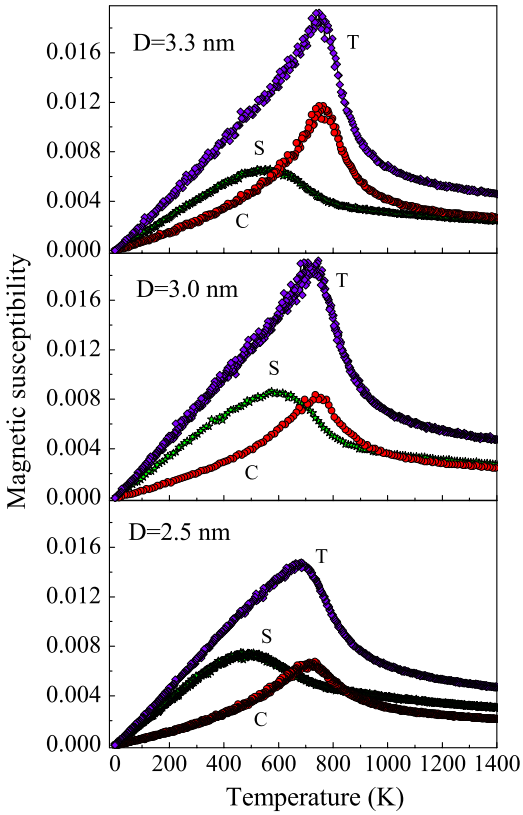

Figure 9. Temperature dependence of the total susceptibility (T), core (C), and surface (S) contributions for diameters of 2.5 nm (bottom), 3.0 nm (middle), and 3.3 nm.

for three different core-to-surface percentages, around 50:50, corresponding to nanoparticles of 2.5, 3.0, and 3.3 nm in diameter. The upward concave behaviour of the core contributions to the total susceptibility below and above the Curie temperature are similar to those found in thermal-driven magnetic phase transitions. For the biggest particle, the susceptibility tends to diverge in the vicinity of the Curie temperature T_C as the bulk system does. In contrast, the surface does not resemble a typical phase transition. Instead of that, a very rounded peak with a maximum shifted to temperatures below T_C is observed. Moreover, a downward concave behaviour is observed below this maximum. Consequently, the total susceptibility becomes less or more rounded around T_C, depending on the relative weight of the surface. The fact that the temperatures at which the surface susceptibility reaches the maximum are lower than those found in the core indicates that both surface and core begin to behave in a different manner. This phenomenology resembles a phase separation process and suggests that the phase transition takes place in a very gradual fashion.

4. Conclusions

The interplay between stoichiometry, particle size, and magnetic properties, has been investigated for magnetite nanoparticles. The particle size dependence of the Curie temperature follows an expression according to the finite size

scaling theory and is characterized by a critical exponent $\nu = 0.82(5)$. Critical temperatures were smaller than that of bulk magnetite due to the presence of dangling bonds on the surface. Results revealed the absence of surface spin disorder or any kind of spin canting phenomenology. Hence, an antiparallel alignment between A and B iron moments over the whole volume of the nanoparticles is concluded. It must be stressed, however, that a higher degree of competition between the surface anisotropy constant and the superexchange integrals could presumably lead to some sort of spin surface canting. Our data also revealed the occurrence of a threshold diameter around 5.0 nm below which off-stoichiometry is increasingly more noticeable and above which nanoparticles can be considered as highly stoichiometric. Finally, the differentiated analysis of the core and surface contributions to the total susceptibility allows us to conclude that both regions behave in a different manner resembling a magnetic phase separation process, and giving rise to a gradual transition. More specifically, susceptibility data suggest a magnetically softer character for the surface relative to the core. Such a hard–soft interplay at the core–surface interface can, presumably, be responsible for the exchange-bias behaviour that has been observed in ferrimagnetic nanoparticles [27, 28].

Acknowledgments

This work was supported through the following grants: COLCIENCIAS-CONICYT Colombia-Chile 2005-206; COLCIENCIAS grant 1115-05-17603, FONDECYT-Chile grant 1050066, Millenium Science Nucleus 'Basic and applied magnetism' P06-022F, grant IN1247CE-CODI of GICM, 'Sostenibilidad GES 2007-2008 E01316' and 'Sostenibilidad GICM 2007-2008 IN1354CE' at Universidad de Antioquia. One of the authors (JM-Z) gratefully acknowledges COLCIENCIAS and Universidad de Antioquia for financial support.

References

[1] Zhang Z and Satpathy S 1991 *Phys. Rev.* B **44** 13319
[2] García J and Subías G 2004 *J. Phys.: Condens. Matter* **16** R145
Piekarz P, Parlinski K and Oles Andrzej M 2006 *Phys. Rev. Lett.* **97** 156402
[3] Zhu L, Yao K L and Liu Z L 2006 *Phys. Rev.* B **74** 035409
[4] Shepherd J P, Koenitzer J W, Aragón R, Spalek J and Honig J M 1991 *Phys. Rev.* B **43** 8461
[5] Honig J M 1995 *J. Alloys Compounds* **229** 24
[6] Poddar P, Fried T and Markovich G 2002 *Phys. Rev.* B **65** 172405
[7] Luo W, Nagel S R, Rosenbaum T F and Rosenweig R E 1991 *Phys. Rev. Lett.* **67** 2721
[8] Lima E Jr, Brandl A L, Arelaro A D and Goya G F 2006 *J. Appl. Phys.* **99** 083908
[9] Morrall P, Schedin F, Case G S, Thomas M F, Dudzik E, van der Laan G and Thornton G 2003 *Phys. Rev.* **67** 214408
[10] Kodama R H and Berkowitz A E 1999 *Phys. Rev.* B **59** 6321
[11] Cornell R M and Schwertmann U 1996 *The Iron Oxides* (Weinheim: VCH)
[12] Martínez-Boubet C *et al* 2006 *Phys. Rev.* B **74** 054430
[13] Gilmore K, Idzerda Yves U, Klem Michael T, Allen M, Douglas T and Young M 2005 *J. Appl. Phys.* **97** 10B301
[14] Goya G F, Berquó T S, Fonseca F C and Morales M P 2003 *J. Appl. Phys.* **94** 3520
[15] Goya G F 2004 *Solid State Commun.* **130** 783–787
[16] Kim T and Shima M 2007 *J. Appl. Phys.* **101** 09M516
[17] Guardia P, Batlle-Brugal B, Roca A G, Iglesias O, Morales M P, Serna C J, Labarta A and Batle X 2007 *J. Magn. Magn. Mater.* **316** e756–9
[18] Wang H, Zhu T, Zhao K, Wang W N, Wang C S, Wang Y J and Zhan W S 2004 *Phys. Rev.* B **70** 092409
[19] Tzitzios V K, Petridis D, Zafirpoulou I, Hadjipanayis G and Niarchos D 2005 *J. Magn. Magn. Mater.* **294** e95–8
[20] Chitu L, Jergel M, Majkova E, Luby S, Capek I, Satka A, Ivan J, Kovac J and Timko M 2007 *Mater. Sci. Eng.* C **27** 1415–7
[21] Tao K, Hongjing D and Sun K 2006 *Colloids Surf.* A **290** 70–6
[22] Zheng R K, Wen G H, Fung K K and Zhang X X 2004 *Phys. Rev.* B **69** 214431
[23] Uhl M and Siberchicot B 1995 *J. Phys.: Condens. Matter* **7** 4227–37
[24] Mazo-Zuluaga J, Restrepo J and Mejía-López J 2007 *Physica* B **398** 187
[25] Landau D P and Binder K 2000 *A Guide to Monte-Carlo Simulations in Statistical Physics* (Cambridge: Cambridge University Press)
[26] Chen K, Ferrenberg Alan M and Landau D P 1993 *Phys. Rev.* B **48** 3249
[27] Nogués J, Sort J, Langlais V, Skumryev V, Suriñach S, Muñoz J S and Baró M D 2005 *Phys. Rep.* **422** 65
[28] Nogués J and Schuller I K 1999 *J. Magn. Magn. Mater.* **192** 203